RadioGraphics

Biliary MR Imaging with Gd-EOB-DTPA and Its Clinical Applications[1]

Nam Kyung Lee, MD • Suk Kim, MD • Jun Woo Lee, MD • Suk Hong Lee, MD • Dae Hwan Kang, MD • Gwang Ha Kim, MD • Hyung Il Seo, MD

TEACHING POINTS
See last page

The hepatocyte-specific contrast agent gadolinium ethoxybenzyl diethylenetriamine pentaacetic acid (Gd-EOB-DTPA) was developed to improve the detection and characterization of focal liver lesions at magnetic resonance (MR) imaging. Approximately 50% of the injected dose is taken up into the functional hepatocyte and is excreted via the biliary system. Because of this property, Gd-EOB-DTPA has the potential to be a biliary contrast agent. When combined with T2-weighted MR cholangiography, Gd-EOB-DTPA–enhanced MR imaging can allow morphologic and functional assessment of the biliary system. Gd-EOB-DTPA–enhanced MR cholangiography could be effective in evaluation of biliary anatomy, differentiation of biliary from extrabiliary lesions, diagnosis of cholecystitis, assessment of bile duct obstruction, detection of bile duct injury including leakage and stricture, evaluation of biliary-enteric anastomoses, postprocedure evaluation, differentiation of biloma from other pathologic conditions, and evaluation of sphincter of Oddi dysfunction. However, the clinical applications of this imaging technique have not yet been fully explored, and further investigations are needed to determine the utility of Gd-EOB-DTPA–enhanced MR cholangiography in a clinical setting.

Abbreviations: ERCP = endoscopic retrograde cholangiopancreatography, Gd-BOPTA = gadobenate dimeglumine, Gd-EOB-DTPA = gadolinium ethoxybenzyl diethylenetriamine pentaacetic acid, GRE = gradient-echo, Mn-DPDP = mangafodipir trisodium, RARE = rapid acquisition with relaxation enhancement, 3D = three-dimensional

RadioGraphics 2009; 29:1707–1724 • **Published online** 10.1148/rg.296095501 • **Content Codes:** GI MR

[1]From the Departments of Radiology (N.K.L., S.K., J.W.L., S.H.L.), Internal Medicine (D.H.K., G.H.K.), and Surgery (H.I.S.), Pusan National University Hospital, Pusan National University School of Medicine and Medical Research Institute, Pusan National University, 1-10 Ami-Dong, Seo-Gu, Busan 602-739, Republic of Korea. Presented as an education exhibit at the 2008 RSNA Annual Meeting. Received January 29, 2009; revision requested March 9; final revision received April 20; accepted April 27. Supported by a grant from the Korea Healthcare Technology R&D Project, Ministry for Health, Welfare, and Family Affairs, Republic of Korea. All authors have no financial relationships to disclose. **Address correspondence to** S.K. (e-mail: *kimsuk@medimail.co.kr*).

Introduction

Hepatocyte-specific magnetic resonance (MR) imaging contrast agents were developed with the aim of improving the detection and characterization of lesions during MR imaging of the liver. These contrast agents include mangafodipir trisodium (Mn-DPDP; Teslascan, GE Healthcare, Oslo, Norway), gadobenate dimeglumine (Gd-BOPTA; MultiHance, Bracco Imaging, Milan, Italy), and gadolinium ethoxybenzyl diethylenetriamine pentaacetic acid (Gd-EOB-DTPA; Primovist, Bayer-Schering Pharma, Berlin, Germany) (1,2). Most previous studies that characterized the use of hepatocyte-specific MR imaging contrast agents have been limited to the detection and characterization of focal liver lesions. Also, few studies have evaluated the use of MR cholangiography with Mn-DPDP (also termed functional MR cholangiography or contrast-enhanced MR cholangiography) as an alternative to conventional T2-weighted MR cholangiography in evaluation of the biliary tree (3–10).

The newly developed hepatocyte-specific MR imaging contrast agent Gd-EOB-DTPA was designed for intravenous use in T1-weighted MR imaging of the liver (1,2,11–18). Gd-EOB-DTPA is a paramagnetic contrast solution that combines the features of an extracellular contrast agent and a hepatocyte-specific agent. Consequently, it is useful in detecting and characterizing lesions in patients known or suspected to have focal or diffuse liver disease (1,2,11–13). However, few studies have evaluated the use of functional MR cholangiography with Gd-EOB-DTPA used as the contrast agent (14,15).

In this article, we briefly review the hepatic kinetics of Gd-EOB-DTPA and compare it to other hepatocyte-specific contrast agents. In addition, we discuss many of the numerous clinical applications of Gd-EOB-DTPA to provide a functional assessment of the biliary system, including its use in evaluation of the biliary anatomy; differentiation of biliary from extrabiliary lesions; diagnosis of acute cholecystitis; assessment of biliary obstruction; evaluation of bile duct injury, biliary-enteric anastomosis, and sphincter of Oddi dysfunction; differentiation of a biloma from other pathologic conditions; and postprocedure evaluation. To prevent misinterpretation of the results obtained with Gd-EOB-DTPA–enhanced MR imaging, we describe the pitfalls that may be encountered with its use.

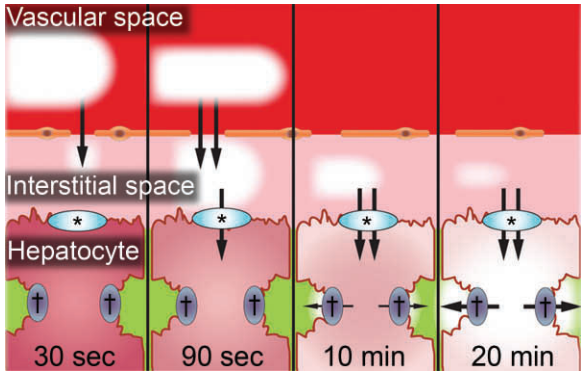

Figure 1. Kinetics of Gd-EOB-DTPA. ∗ = organic anion transport system, † = adenosine triphosphate–dependent glutathione S-transferase.

Kinetics of Gd-EOB-DTPA

Teaching Point

Gd-EOB-DTPA is a highly water-soluble contrast agent in which an ethobenzyl group is attached to gadolinium diethylenetriamine pentaacetic acid. The resulting compound has the properties of a conventional nonspecific extracellular contrast agent but with the additional properties of a hepatocyte-specific agent, thereby allowing improved examination of the hepatobiliary system (1,2,11–18).

When Gd-EOB-DTPA is injected intravenously as a bolus, its blood pool properties are transient and less intense than those of an extracellular contrast agent, so that early dynamic imaging is possible. The basic principle of early dynamic phase imaging with Gd-EOB-DPTA is the same as that for use of gadolinium-based nonspecific extracellular contrast agents. However, the T1 relaxivity of Gd-EOB-DTPA in blood (7.3 L/mmol·sec) is higher than that of standard gadolinium chelates (around 4.5 L/mmol·sec) owing to the weak protein binding of Gd-EOB-DTPA, resulting in a lower gadolinium concentration of Gd-EOB-DPTA (0.25 mol/L) compared with that of other standard gadolinium chelates (0.5 mol/L). The recommended dose (0.025 mmol/kg of body weight) is also lower than that of gadolinium chelates (0.1 mmol/kg of body weight) (19).

Owing to the presence of the lipophilic ethobenzyl group, Gd-EOB-DTPA readily enters hepatocytes via an organic anion transport system and is excreted into the biliary system by an adenosine triphosphate–dependent glutathione S-transferase that requires adenosine triphosphate for activity (Fig 1). Intense enhancement of the liver during the delayed hepatobiliary phase can be obtained after 20 minutes and lasts for at least 120 minutes after Gd-EOB-DTPA injection (1,2,11–13). Intense enhancement of bile within the common bile duct has been reported to begin as early as 10 minutes after contrast material administration in healthy volunteers, and a 20-minute delay after Gd-EOB-DTPA injection may be sufficient for adequate biliary evaluation (14–16).

Gd-EOB-DTPA is eliminated in the nonmetabolized form in approximately equal proportions via biliary excretion (43.1%–53.2%) and renal glomerular filtration with subsequent excretion (41.6%–51.2%) (2,11,12). Because Gd-EOB-DTPA uptake is mediated by the same transporter responsible for bilirubin transport, biliary obstruction or diminished hepatobiliary function can be suspected in patients with reduced or no visualization of the biliary tree 20–30 minutes after Gd-EOB-DTPA administration (17).

Comparison of Hepatocyte-specific Contrast Agents

Mn-DPDP is a pure hepatocyte-specific agent, whereas Gd-BOPTA and Gd-EOB-DTPA combine the properties of a conventional nonspecific extracellular contrast agent and a hepatocyte-specific agent (1,2). Mn-DPDP was the first clinically available hepatocyte-specific contrast agent mostly eliminated through the biliary system (45%–55%). Maximum liver enhancement is observed within 10–15 minutes after infusion. However, dynamic imaging with Mn-DPDP is not possible because the T1 relaxivity of the agent in blood is less than that of gadolinium chelates (1,2).

Gd-BOPTA and Gd-EOB-DTPA can be used as intravascular-interstitial contrast agents for dynamic MR imaging and as hepatocyte-specific contrast agents yielding prolonged enhancement of the liver. Unlike with Gd-EOB-DTPA, approximately 5% of the administered dose of Gd-BOPTA is excreted in the bile while the remainder is excreted by the kidney (1,2). The optimal window for evaluating the liver parenchyma and bile duct after injection ranges from 10 to 20 minutes for Gd-EOB-DTPA and from 60 to 120 minutes for Gd-BOPTA. Therefore, Gd-EOB-DTPA may provide adequate biliary imaging within a shorter time than Gd-BOPTA (18).

MR Imaging Technique

At our institution, MR imaging is performed with superconductive 3.0-T and 1.5-T imaging units (Magnetom Trio and Sonata, respectively; Siemens Medical Solutions, Erlangen, Germany) and a phased-array multicoil. Initially, conventional T2-weighted MR cholangiography was performed before administration of intravenous Gd-EOB-DTPA to prevent the T2-shortening effect of the concentrated contrast agent within the bile ducts. Two MR cholangiographic techniques are used: multiple-section thin-collimation half-Fourier rapid acquisition with relaxation enhancement (RARE) sequences performed in the coronal and oblique projections and thick-slab single-shot echo-train spin-echo sequences performed in the coronal plane.

Subsequent Gd-EOB-DTPA–enhanced MR images that included early dynamic phase and delayed hepatobiliary phase images were acquired by using axial or coronal dynamic three-dimensional (3D) gradient-echo (GRE) (volume-interpolated breath-hold examination) imaging. The imaging parameters of the T1-weighted 3D GRE sequences were as follows: 3.6/1.4 (repetition time msec/echo time msec), 10° flip angle, 3-mm slab thickness with no gap, 360 × 320-mm field of view, 256 × 115 or 256 × 134 matrix, and 18-second acquisition time. Each patient who underwent imaging received an intravenous bolus injection of Gd-EOB-DTPA as a contrast agent at a dose of 25 μmol/kg of body weight and a flow rate of 1–2 mL/sec, followed by injection of 20 mL of sterile saline solution. The safety and efficacy of Gd-EOB-DTPA have not been established in patients under 18 years old.

For the early dynamic phase, the initial sequence was performed before contrast agent administration. To minimize interindividual differences in circulation time, arterial phase imaging was started manually by using the bolus tracking technique at the time the contrast agent reached the abdominal aorta, typically 5–10 seconds after the start of injection. Portal venous phase and equilibrium phase images were acquired 45 and

Figure 2. Medial insertion of the cystic duct in a 60-year-old man. **(a)** On a coronal T2-weighted RARE image, the cystic duct appears as a lateral insertion (arrow). **(b)** Coronal multiplanar reformation Gd-EOB-DTPA–enhanced T1-weighted 3D GRE image obtained 60 minutes after injection shows a medial insertion of the cystic duct (arrow). Gd-EOB-DTPA–enhanced MR cholangiography provides better delineation of the bile duct compared with that provided by conventional MR cholangiography.

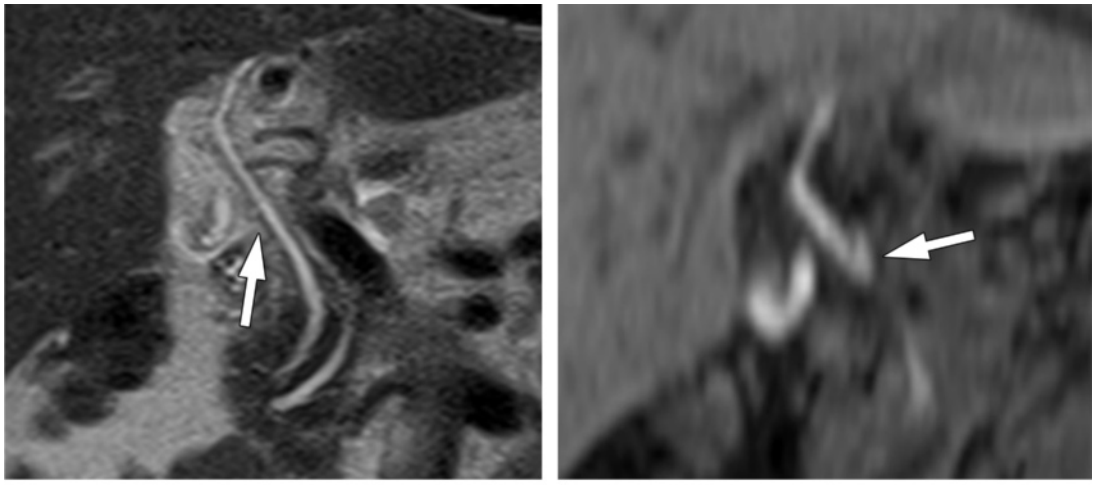

a. b.

Figure 4. Choledochal cyst in a 41-year-old woman. **(a)** Coronal T2-weighted RARE image shows a bile duct with a long common channel (arrowhead) and saccular dilatation (arrow). This appearance is indicative of a choledochal cyst, which resembles an extrabiliary cystic lesion. **(b)** Coronal multiplanar reformation Gd-EOB-DTPA–enhanced T1-weighted 3D GRE image obtained 60 minutes after injection shows contrast material filling the saccular dilated bile duct (*) in continuity with the distal duct.

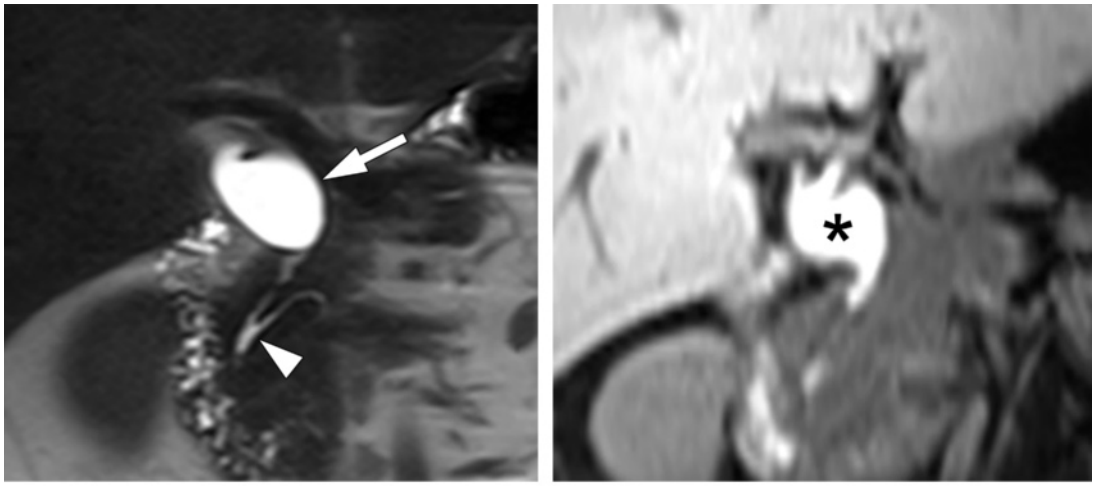

a. b.

90 seconds and 5 minutes after contrast agent administration. Hepatobiliary phase images were acquired 10, 20, 30, and 60 minutes after contrast agent administration. Additional delayed MR images from a time more than 60 minutes after bolus administration of Gd-EOB-DTPA were obtained if visualization of the bile ducts was not sufficient for anatomic diagnosis within 60 minutes after contrast agent administration.

Clinical Applications

Biliary Anatomy and Anatomic Variants

Anatomic variation of the biliary tree is seen in approximately 30% of patients and is a known risk factor for bile duct injury during hepatobiliary surgery (20–22). MR cholangiography is a

Figure 3. Bile leak after laparoscopic cholecystectomy in a 72-year-old woman. The bile leak was due to transection without ligation of an aberrant right hepatic duct (Strasberg classification type C). **(a)** Coronal T2-weighted RARE image obtained 21 days after laparoscopic cholecystectomy shows abrupt cutoff of an aberrant right hepatic duct (arrow). **(b)** Gd-EOB-DTPA–enhanced 3D GRE T1-weighted image obtained 60 minutes after injection shows extravasation of contrast material from the aberrant right hepatic duct (arrow) into the gallbladder bed (arrowhead). **(c)** Image from endoscopic retrograde cholangiopancreatography (ERCP) shows no filling of the aberrant right hepatic duct and no apparent bile leak. The reasons for these findings are because the aberrant right hepatic duct was divided at the original surgery and the cystic duct remnant was surgically closed with clips.

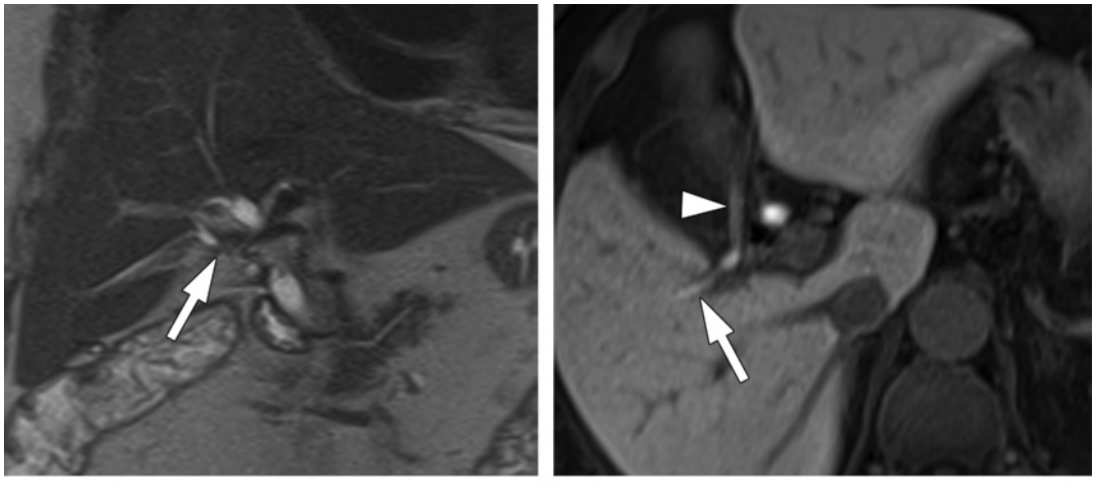

a. b.

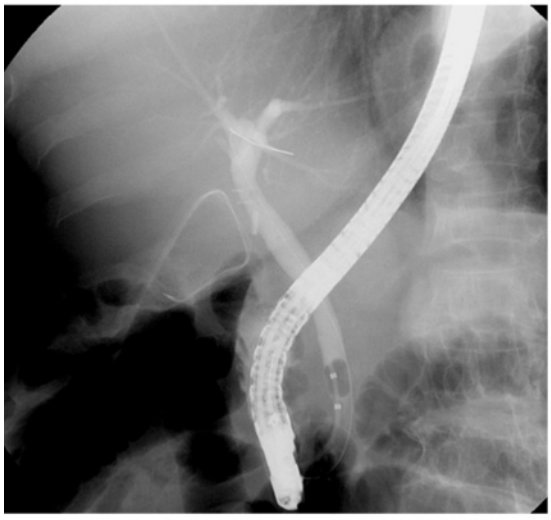

c.

noninvasive method for demonstrating anatomic variations of the biliary tree, such as a low or medial insertion of the cystic duct and an aberrant right hepatic duct (20,23).

Gd-EOB-DTPA–enhanced MR imaging provides a higher signal-to-noise ratio in the bile duct than is achieved with T2-weighted MR cholangiography, resulting in better delineation of bile duct anatomy, particularly in the intrahepatic bile ducts, even if the bile ducts are not dilated (Fig 2) (6,7,15,24). Therefore, Gd-EOB-DTPA–enhanced MR imaging combined with conventional T2-weighted MR cholangiography can be helpful in identifying the course of anatomic variations of the biliary tree and bile duct injuries related to these variations before or after surgery (Fig 3) (6,7,15,24).

Differentiation of Biliary from Extrabiliary Lesions

MR cholangiography usually demonstrates the relationship between extrabiliary cystic lesions and bile ducts by delineating the course of the latter. However, unlike direct cholangiography, MR cholangiography does not allow easy distinction between cystic lesions near bile ducts and the bile duct lumen. This drawback is especially true in thick-slab MR cholangiography; separation of cystic lesions from the bile ducts themselves is more difficult with that technique than with thin-section source imaging.

Contrast material, which can be identified on images obtained more than 20 minutes after Gd-EOB-DTPA administration, can opacify and distend the lumen of the biliary tract. Therefore, it may be useful in the demonstration of cystic abnormalities that communicate with the bile ducts and facilitate differentiation of a choledochal cyst from extrabiliary cystic lesions, such as pseudocyst, duodenal diverticulum, or duodenal duplication, which do not communicate with the bile ducts (Figs 4, 5) (6,25).

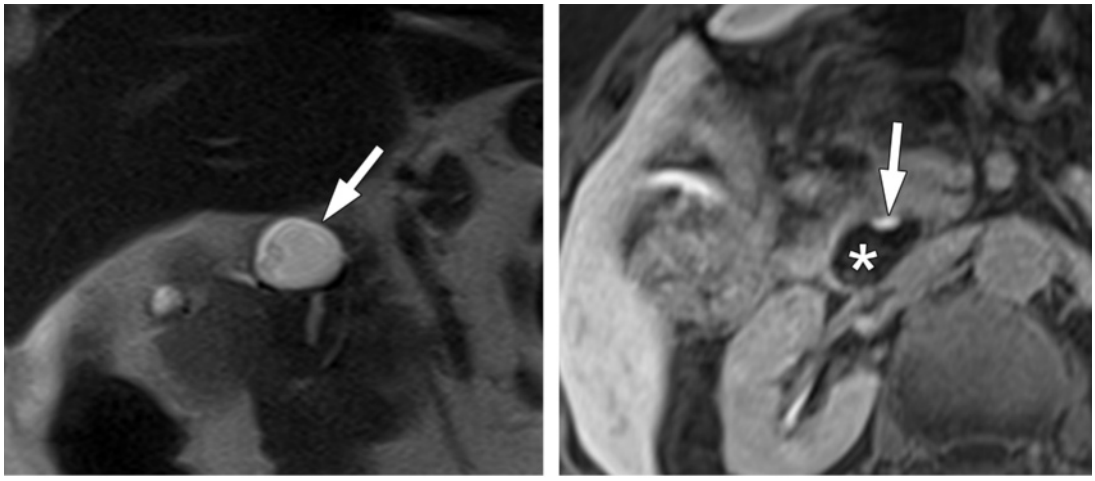

a. b.

Figure 5. Periampullary diverticulum in a 75-year-old woman. **(a)** Coronal T2-weighted RARE image shows a well-defined, round cystic lesion (arrow) that is closely related to the common bile duct, duodenum, and pancreatic head. **(b)** Axial Gd-EOB-DTPA–enhanced T1-weighted 3D GRE image obtained 60 minutes after injection shows no communication between the cystic lesion (*) and the enhancing common bile duct (arrow). The diagnosis of a periampullary diverticulum was made with endoscopy.

Because the pancreatic duct is not visualized at Gd-EOB-DTPA–enhanced MR imaging, this technique is limited in evaluating the relationship between a cystic lesion located adjacent to the pancreatic head and the pancreatic duct. However, Gd-EOB-DTPA–enhanced MR imaging combined with T2-weighted MR cholangiography may have a role in the differentiation of biliary from extrabiliary lesions when results of conventional MR cholangiography are inconclusive or diagnostically insufficient (6).

Caroli disease can be either focal or diffuse. Diffuse Caroli disease should be differentiated from autosomal-dominant polycystic liver disease or peribiliary cysts in a cirrhotic liver. MR imaging findings of Caroli disease include multiple intrahepatic cysts in close relation to the biliary system and the presence of the central dot sign (26). However, MR imaging fails to demonstrate communication between cystic lesions and draining bile ducts. This problem could be resolved with Gd-EOB-DTPA–enhanced MR cholangiography, which can demonstrate communications between cystic lesions and draining bile ducts and allows differentiation of Caroli disease from autosomal-dominant polycystic liver disease or peribiliary cysts in a cirrhotic liver (Figs 6, 7) (6,27,28).

Teaching Point

Acute Cholecystitis

In patients clinically suspected to have acute cholecystitis, ultrasonography (US) is usually favored as the initial imaging technique (29). In a meta-analysis, US was shown to demonstrate acute cholecystitis with a sensitivity of 88% and specificity of 80% (29). Computed tomography (CT) and MR imaging usually provide morphologic information similar to that provided by US and can be performed initially if the clinical presentation is atypical. CT and MR imaging are also effective for evaluating suspected complications of acute cholecystitis, such as perforation or abscess, and concurrent intraabdominal conditions (30).

Increased wall enhancement of the gallbladder and increased pericholecystic hepatic parenchymal enhancement are frequent and specific CT and MR imaging findings of acute cholecystitis (31). However, CT and MR imaging in assessment of acute cholecystitis have focused on the detectability of impacted calculi in the cystic duct or gallbladder neck, but cannot depict the dynamics of bile. Biliary scintigraphy is a sensitive method in diagnosis of acute cholecystitis because it is able to demonstrate nonfilling of the gallbladder. However, scintigraphy is now rarely used for this purpose because it cannot provide anatomic information on the biliary system or information about the presence of stones (32).

Previous studies have shown that Mn-DPDP–enhanced MR imaging combined with T2-weighed MR cholangiography is better for detec-

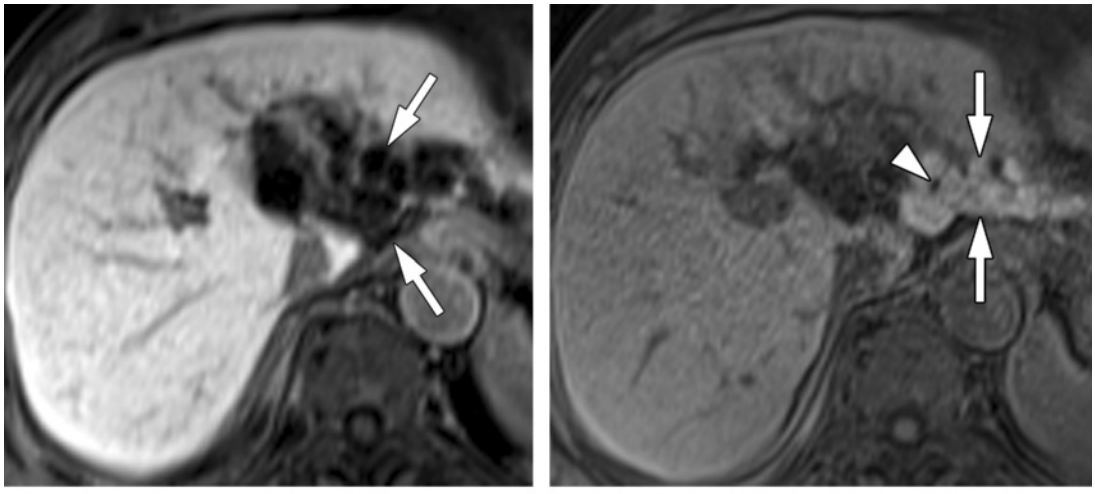

a. b.

Figure 6. Caroli disease in a 68-year-old man. **(a)** Axial Gd-EOB-DTPA–enhanced T1-weighted 3D GRE image obtained during the portal venous phase shows multiple intrahepatic cysts (arrows) in close relation to the biliary system. This finding can be seen in patients with polycystic liver disease, peribiliary cysts in a cirrhotic liver, or diffuse Caroli disease. **(b)** Axial Gd-EOB-DTPA–enhanced T1-weighted 3D GRE image obtained 24 hours after injection shows contrast material filling the cystic lesions (arrows), a finding indicative of communication between the cystic lesions and the bile duct. The contrast material–filled lesions surround a dot-like filling defect (central dot sign) (arrowhead), which represents the central fibrovascular bundle.

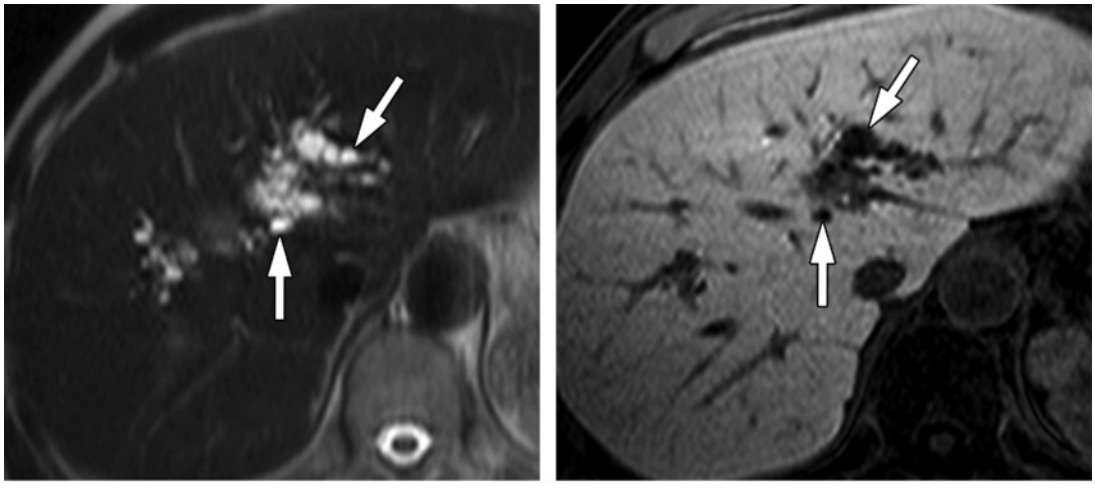

a. b.

Figure 7. Polycystic liver disease in a 53-year-old man. **(a)** Axial T2-weighted RARE image shows multiple intrahepatic cysts (arrows) in close relation to the biliary system. This finding can be seen in patients with polycystic liver disease, peribiliary cysts in a cirrhotic liver, or diffuse Caroli disease. **(b)** Axial Gd-EOB-DTPA–enhanced T1-weighted 3D GRE image obtained 60 minutes after injection shows no communication between the cystic lesions (arrows) and the bile duct in the noncirrhotic liver.

tion of acute cholecystitis as nonvisualization of contrast material filling in the gallbladder than is conventional T2-weighted MR cholangiography (3,8). Mn-DPDP–enhanced MR imaging combined with T2-weighed MR cholangiography could be useful for evaluation of acute cholecystitis, especially when evidence of cystic duct obstruction at T2-weighted MR cholangiography is equivocal or negative but clinical suspicion is high.

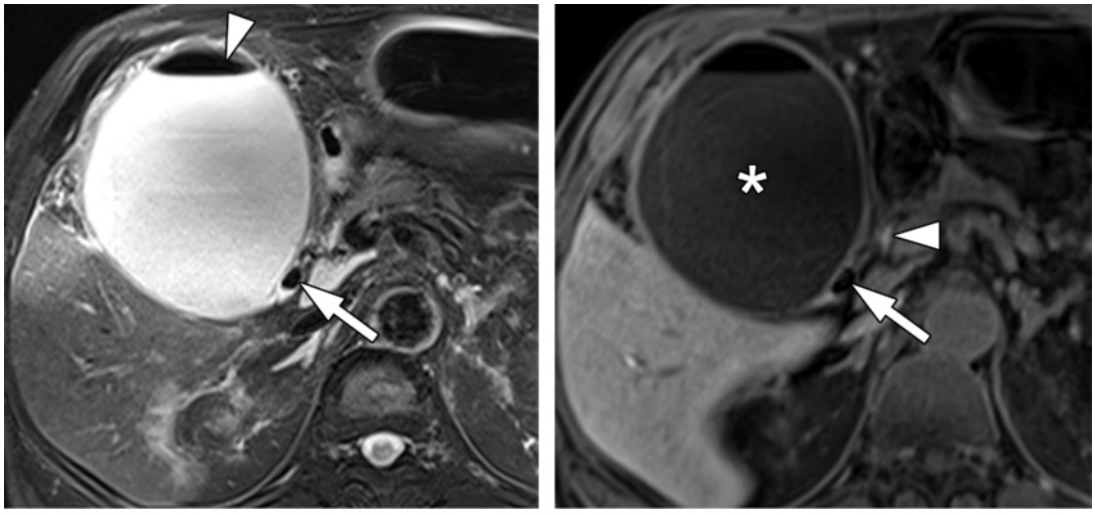

a. b.

Figure 8. Acute calculous cholecystitis in a 69-year-old man. **(a)** Axial T2-weighted turbo spin-echo image shows a markedly distended gallbladder and mild hypointense thickening of the gallbladder wall. A stone in the gallbladder neck appears as a filling defect (arrow). The air in the nondependent portion of the gallbladder (arrowhead) is due to previous endoscopic stone removal. **(b)** Axial Gd-EOB-DTPA–enhanced T1-weighted 3D GRE image obtained 60 minutes after injection shows no opacification of the distended gallbladder by contrast material (*), whereas the extrahepatic duct is enhanced (arrowhead). These findings are indicative of a functional obstruction in the gallbladder neck. Note the signal void of the stone in the gallbladder neck (arrow).

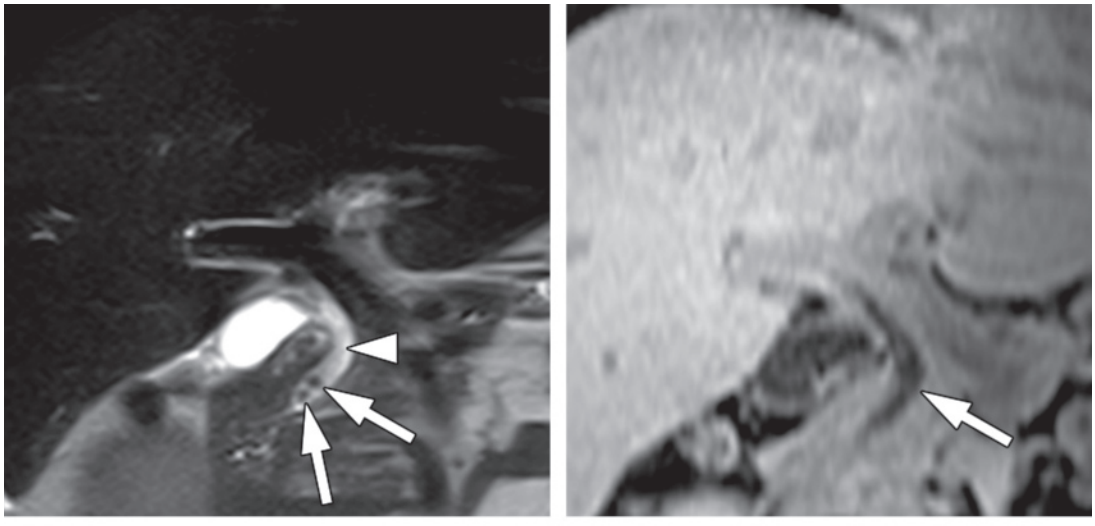

a. b.

Figure 9. Distal common bile duct stones in a 48-year-old man. The patient's serum bilirubin level was elevated (3.1 mg/dL [53.0 μmol/L]). **(a)** Coronal T2-weighted RARE image shows two stones (arrows) and plug-like sludge or pus with a fluid-fluid level (arrowhead) in the distal common bile duct and mild dilatation of the upstream duct. **(b)** Coronal multiplanar reformation Gd-EOB-DTPA–enhanced T1-weighted 3D GRE image obtained 60 minutes after injection shows no excretion of contrast material into the biliary tree in the intrahepatic or extrahepatic ducts (arrow), a finding indicative of complete obstruction or severe hepatic dysfunction related to stones. **(c)** Photograph obtained during an endoscopic procedure for stone removal shows pus (*) leaking from the papilla, a finding indicative of suppurative cholangitis.

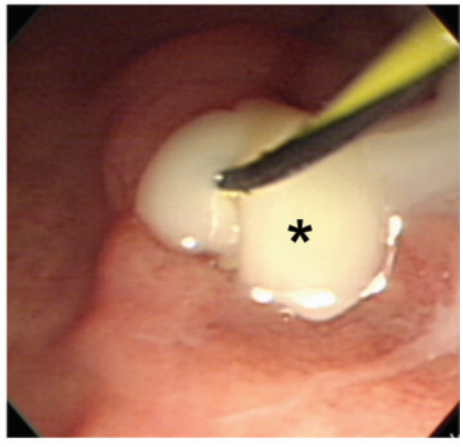

c.

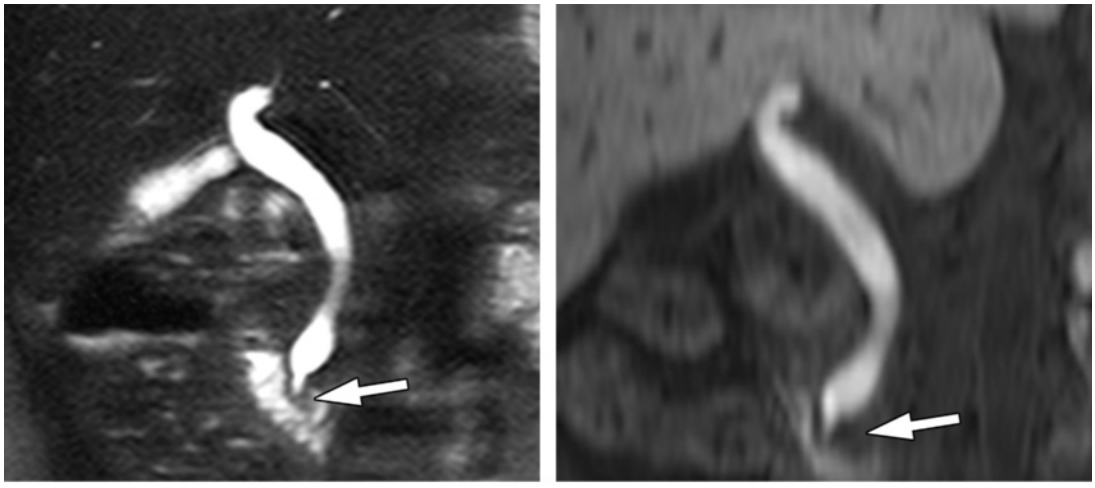

a. b.

Figure 10. Ampullary carcinoma with partial obstruction in a 50-year-old woman. **(a)** Coronal T2-weighted RARE image shows a bulging ampulla and irregularly thickened ampullary mucosa (arrow) with upstream bile duct dilatation. **(b)** Coronal multiplanar reformation Gd-EOB-DTPA–enhanced T1-weighted 3D GRE image obtained 60 minutes after injection shows bulging of the papilla with asymmetric wall thickening (arrow). Note the dilated extrahepatic duct and the excretion of contrast material into the duodenum, findings indicative of partial obstruction. The mass was diagnosed after surgical resection as an ampullary carcinoma.

To our knowledge, there are no published studies on use of Gd-EOB-DTPA–enhanced MR imaging for diagnosis of acute cholecystitis. However, in our experience, Gd-EOB-DTPA–enhanced MR imaging combined with T2-weighted MR cholangiography could also improve the ability to diagnose acute cholecystitis by providing not only anatomic information such as an impacted cystic duct or gallbladder stones, but also functional information on cystic duct obstruction as evidenced by lack of visualization of contrast material filling in the gallbladder, similar to the information provided by Mn-DPDP–enhanced MR imaging (Fig 8) (3,8).

Teaching Point

Bile Duct Obstruction

MR cholangiography is highly accurate in diagnosis of the presence and level of bile duct obstruction, but this imaging technique cannot effectively demonstrate the degree of bile duct obstruction (33). However, if hepatocyte-specific contrast agents are used, MR cholangiography could offer reliable information on bile flow dynamics (4).

Although the biliary excretion of Gd-EOB-DTPA may be affected by various factors as well as the degree of bile duct obstruction, the degree of bile duct obstruction might be simply classified with delayed Gd-EOB-DTPA–enhanced bile flow dynamics (usually evaluated >30 minutes after intravenous injection of Gd-EOB-DTPA): complete obstruction (absence of contrast agent filling in the distal and even proximal parts of the stricture or obstructive lesion), near-complete obstruction (significantly delayed contrast agent filling only in the proximal part of the stricture or obstructive lesion), and partial obstruction (passage of contrast agent beyond the apparent stricture or obstructive lesion) (Figs 9, 10) (4–6,16). The distinction between complete and partial obstruction of the bile duct may affect the therapeutic approach as well as the timing of further treatment, particularly in patients suspected to have cholangitis or biliary stricture after cholecystectomy (34).

Teaching Point

Gd-EOB-DTPA–enhanced MR cholangiography may also be useful for assessment of regional morphologic and functional impairments due to malignant hilar obstruction. The severity of the obstructed ductal segment might be determined by observing passage of the contrast material through the malignant stricture on Gd-EOB-DTPA–enhanced MR images. This finding may be important in assessment of a specific segment of a duct scheduled for endoscopic or percutaneous palliative drainage in patients with unresectable malignant hilar obstructions (Fig 11) (35). However, the role of Gd-EOB-DTPA–enhanced MR imaging in assessment of regional impairments due to malignant obstruction has not yet been established, and further studies are needed to determine its role in clinical practice.

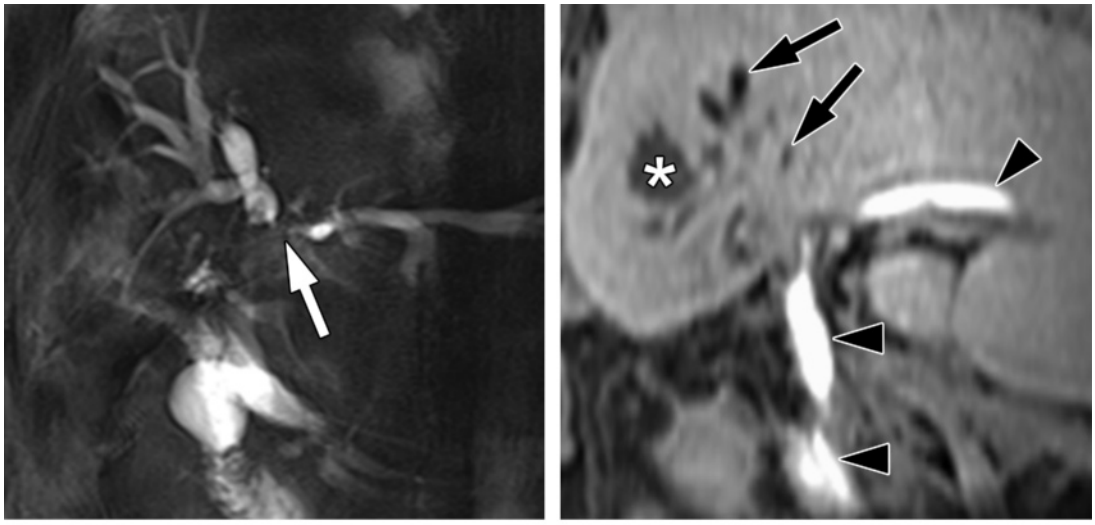

a. b.

Figure 11. Hilar cholangiocarcinoma (Bismuth type IIIa) in a 64-year-old man. **(a)** Coronal image from thick-slab single-shot MR cholangiography shows intrahepatic duct dilatation and obstruction at the porta hepatis (arrow). **(b)** Coronal multiplanar reformation Gd-EOB-DTPA–enhanced T1-weighted 3D GRE image obtained 60 minutes after injection shows absence of contrast material filling in the right intrahepatic ducts (arrows), a finding consistent with complete or near-complete obstruction. Conversely, contrast material is seen in the left intrahepatic ducts with excretion into the common bile duct and duodenum (arrowheads), a finding indicative of partial obstruction. Note the liver abscess (*).

Bile Duct Injury

Bile duct injuries are the most common and serious complications associated with surgery, especially laparoscopic cholecystectomy. The reported rate of bile duct injury ranges from 0.4% to 0.8% for laparoscopic cholecystectomy versus 0.1% to 0.3% for open cholecystectomy (36,37).

Traditionally, bile duct injuries have been classified by using the Bismuth or Strasberg classification. The Bismuth classification is based on the localization of biliary strictures according to the distance from the biliary confluence but does not encompass the entire spectrum of bile duct injury. Therefore, Strasberg et al (37) made the Bismuth classification much more comprehensive by including other types of laparoscopic extrahepatic bile duct injury (Table) (38). Type A, the most common form of bile duct injury, is seen after laparoscopic cholecystectomy and involves leakage from the cystic duct or the bile ducts of Luschka (Fig 12). The latter are accessory tiny bile ducts that run along the gallbladder fossa and commonly drain into the right hepatic duct (37,39).

Bile leaks usually manifest within the first postoperative week, whereas strictures without a bile leak tend to manifest several months to years after surgery. Persistent and profuse bile secretion from a surgically placed drain in association with pain and fever together with varying degrees of distention, ileus, and jaundice are hallmarks of a significant bile leak. Such patients usually have signs of biliary obstruction as well (21).

In patients suspected to have a bile leak, cross-sectional imaging studies are useful in depicting the presence of a fluid collection in the gallbladder bed or perihepatic region. However, these studies cannot demonstrate communication between the fluid collection and the biliary tree (40). Biliary scintigraphy is a useful tool for confirming the presence of a bile leak and showing the primary course of biliary excretion, but it cannot provide accurate anatomic details (32).

Strasberg Classification of Bile Duct Injuries

Type	Criteria
A	Leaks from the cystic duct or the bile ducts of Luschka
B	Occlusion of aberrant right hepatic ducts
C	Transection without ligation of aberrant right hepatic ducts
D	Lateral injuries to major bile ducts
E	Subdivided per the Bismuth classification into E1–E5

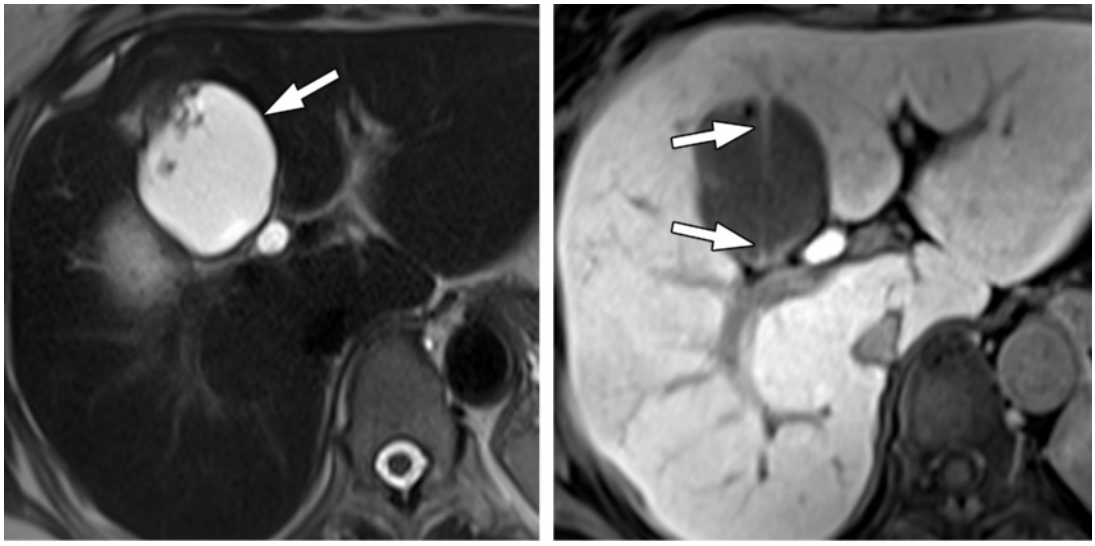

a. b.

Figure 12. Bile leak (Strasberg classification type A) after laparoscopic cholecystectomy in a 58-year-old woman. **(a)** Axial T2-weighted RARE image obtained 45 days after laparoscopic cholecystectomy shows a loculated fluid collection (arrow) at the gallbladder bed. **(b)** Gd-EOB-DTPA–enhanced T1-weighted 3D GRE image obtained 60 minutes after injection shows a jet of contrast material (arrows) within the loculated fluid collection, an appearance indicative of a bile leak from the bile duct of Luschka.

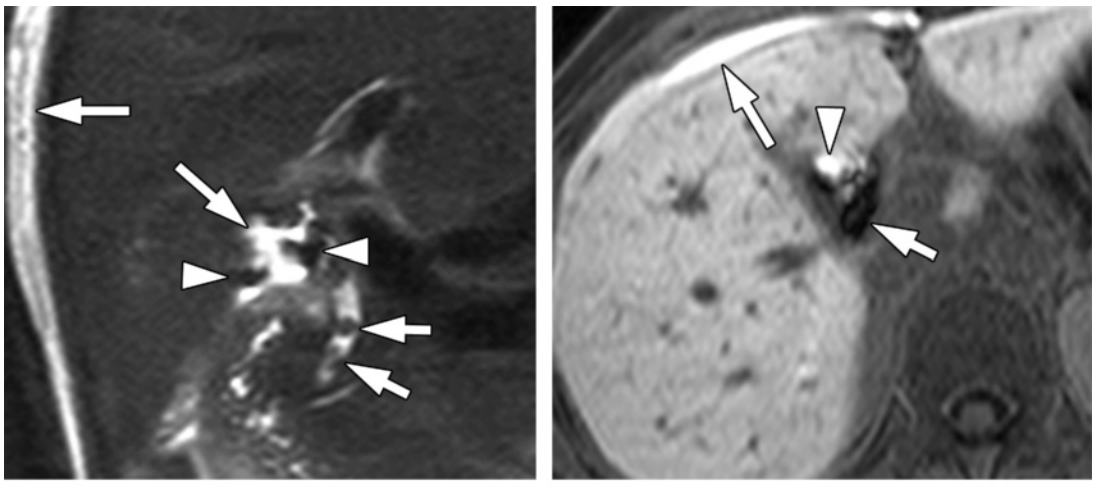

a. b.

Figure 13. Bile leak after laparoscopic cholecystectomy in a 26-year-old woman who presented with abdominal pain. **(a)** Coronal T2-weighted RARE image obtained 1 week after cholecystectomy shows small fluid collections in the gallbladder bed and perihepatic space (long arrows). Note the signal void due to the surgical clip (arrowheads) and multiple stones in the common bile duct (short arrows). **(b)** Gd-EOB-DTPA–enhanced T1-weighted 3D GRE image obtained 60 minutes after injection shows extravasation of contrast material from the cholecystectomy bed (arrowhead) into the perihepatic space (long arrow). Note the signal void due to the surgical clip (short arrow).

Teaching Point

Gd-EOB-DTPA–enhanced MR cholangiography allows detection of active bile leakage by direct visualization of contrast material extravasating into fluid collections, as well as demonstrating the anatomic site of the leakage and the type of bile duct injury (Figs 3, 12–14) (22,40). Gd-EOB-DTPA–enhanced MR cholangiography is also useful in assessing the degree of any obstruction according to the presence or absence of contrast material downstream in the bile duct (Fig 14). In patients with complete obstruction of

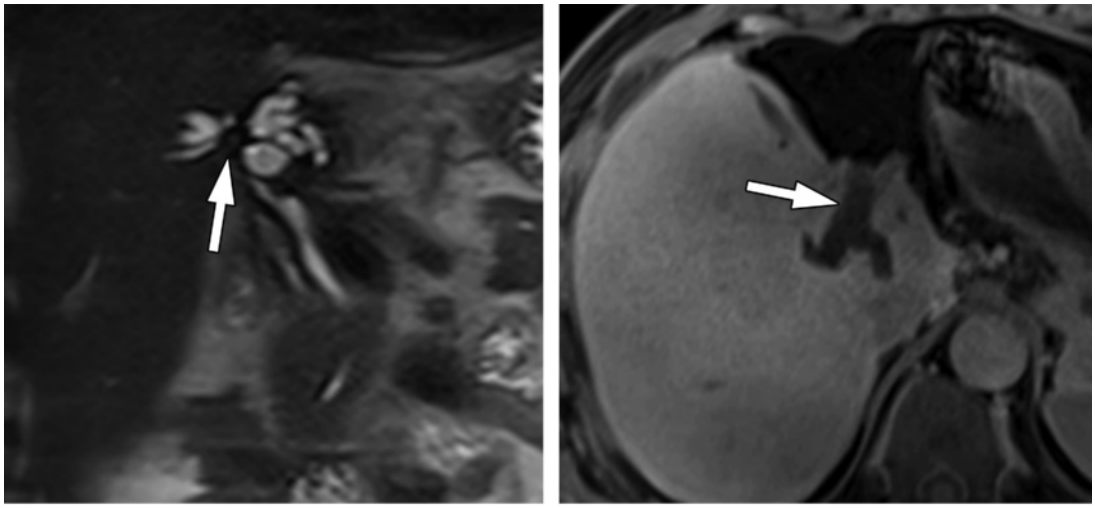

a. b.

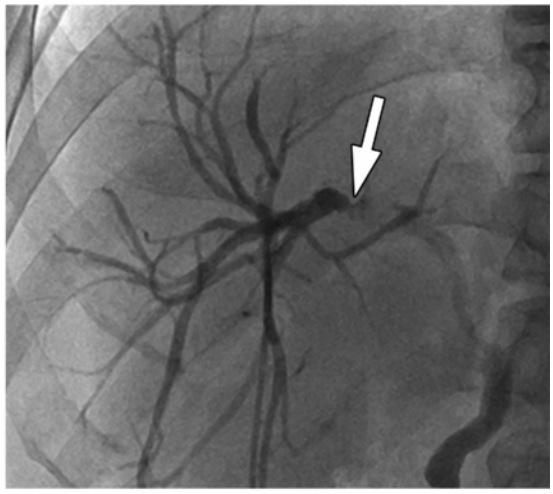

c.

Figure 14. Bile duct stricture due to intrahepatic duct stones 3 years after left lobectomy in a 50-year-old man who presented with jaundice. The patient's serum bilirubin level was elevated (12.43 mg/dL [212.6 μmol/L]). **(a)** Coronal T2-weighted RARE image shows a stricture (arrow) and dilatation of the proximal intrahepatic ducts. **(b)** Gd-EOB-DTPA–enhanced T1-weighted 3D GRE image obtained 60 minutes after injection shows no excretion of contrast material into the right main hepatic duct (arrow). **(c)** Image from direct cholangiography shows the high-grade stricture (arrow) of the right main hepatic duct.

the bile duct after surgery, Gd-EOB-DTPA–enhanced MR imaging shows a stricture or transection at or around the surgical clips, with proximal duct dilatation and lack of excretion of the contrast agent from the bile duct (Fig 14) (22,40).

Gd-EOB-DTPA–enhanced MR cholangiography can be useful for planning the appropriate treatment because it can demonstrate the primary course of biliary excretion. Patients with a bile leak but without significant major duct injury usually do not require intervention, but percutaneous external drainage of the biloma, ERCP with a sphincterotomy, or placement of a stent may be necessary. A major bile duct injury with or without significant bile leak requires more invasive therapy, such as surgical biliary reconstruction (22,40).

Biliary-Enteric Anastomosis

An obstruction is a relatively common complication of a biliary-enteric bypass procedure, occurring in up to about 20% of patients. Direct cholangiography or biliary scintigraphy is used to evaluate a biliary-enteric anastomosis in the treatment of obstruction (41). Biliary scintigraphy does not offer sufficient anatomic information about the anastomosis, and ERCP is difficult to perform in patients with altered surgical anatomy. As an alternative, MR cholangiography is used when the anastomosis cannot be cannulated endoscopically (42).

MR cholangiography depicts the site of biliary-enteric anastomosis, the cause of obstruction, and the status of the biliary ducts upstream (43). However, differentiation between nonobstructive dilatation of the bile ducts with patent anastomoses versus biliary obstruction may be difficult because the technique provides no functional information about biliary drainage (43). Instead, contrast material filling of the bowel loop at Mn-DPDP–enhanced MR cholangiography provides direct evidence of the patency of the biliary-enteric anastomosis. Like-

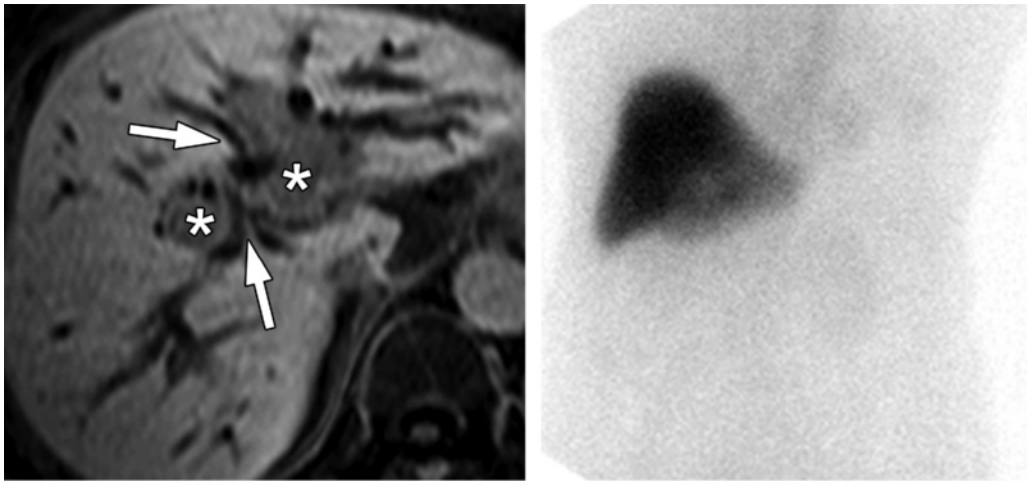

a. b.

Figure 15. Postoperative obstruction at a Roux-en-Y hepaticojejunostomy site in a 63-year-old woman who underwent hepaticojejunostomy because of extrahepatic cholangiocarcinoma. The patient's serum bilirubin level was elevated (4.09 mg/dL [70.0 μmol/L]). **(a)** Eight-month follow-up axial Gd-EOB-DTPA–enhanced T1-weighted 3D GRE image obtained 60 minutes after injection shows mildly dilated intrahepatic ducts without excretion of contrast material into the ducts (arrows), findings consistent with complete obstruction. ∗ = portal vein. Local recurrence was not noted during the follow-up period. **(b)** Image from technetium 99m–diisopropyl iminodiacetic acid scanning, obtained at 5 hours, shows persistent hepatic uptake of the radiotracer without transit into the hepaticojejunostomy site, findings consistent with complete obstruction.

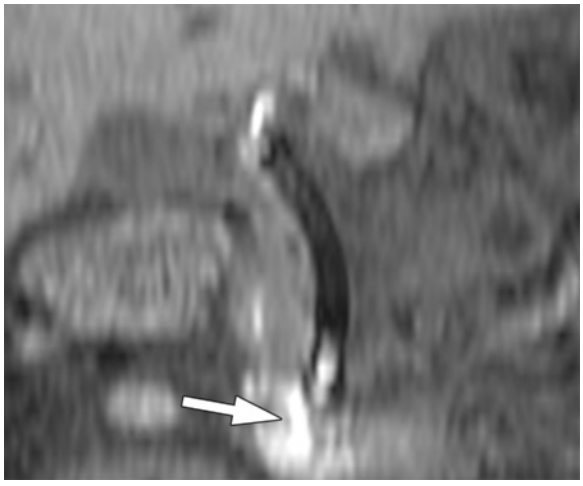

Figure 16. Cancer of the pancreatic head in a 60-year-old woman. The patient underwent placement of a metallic stent across the common bile duct. Coronal multiplanar reformation Gd-EOB-DTPA–enhanced T1-weighted 3D GRE image obtained 60 minutes after injection shows excretion of contrast material through the stent and into the duodenum (arrow).

wise, by using Gd-EOB-DTPA–enhanced MR cholangiography, comprehensive information on the patency of biliary-enteric anastomoses is obtained (Fig 15) (6,10).

Postprocedure Evaluation

After endoscopic or percutaneous radiologic stent implantation in the bile duct, regular follow-up is required to detect stent restenosis or stent dislocation. However, stent imaging continues to be a challenge for cross-sectional imaging approaches. The capabilities of US are diminished owing to difficulty in penetrating the stent cage. Although the absence of proximal dilatation at T2-weighted MR cholangiography may suggest biliary stent patency, MR cholangiography is also not the preferred method for assessing the patency of a metallic stent.

Owing to susceptibility artifacts generated by the metallic stent, MR cholangiography cannot show its exact position or its internal lumen. Susceptibility artifacts created by the metallic stent occur with all MR imaging sequences (44,45). Despite the susceptibility artifacts, Gd-EOB-DTPA–enhanced MR cholangiography, unlike conventional MR cholangiography, allows assessment of stent patency by means of direct visualization of hepatocyte-specific contrast material above and below the stent (Fig 16) (5).

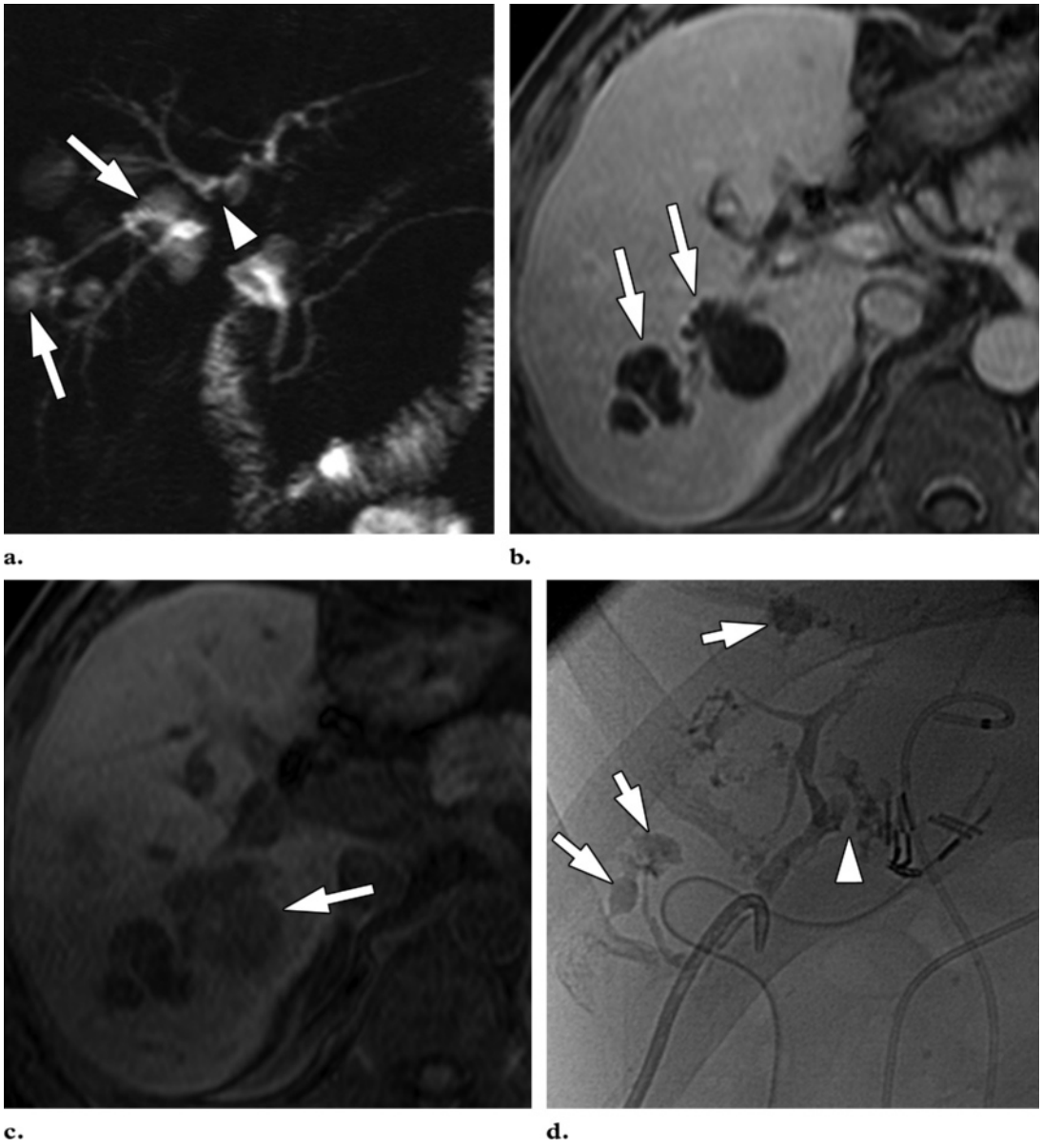

Figure 17. Bile duct injury and multiple bilomas after laparoscopic cholecystectomy in a 47-year-old man. **(a)** Image from coronal thick-slab single-shot MR cholangiography, performed 1 month after laparoscopic cholecystectomy, shows multiple hyperintense lesions (arrows) in the right lobe of the liver and abrupt cutoff of the common hepatic duct (arrowhead) around surgical clips. **(b)** Axial Gd-EOB-DTPA–enhanced T1-weighted 3D GRE image obtained during the portal venous phase shows the well-defined hypointense lesions with thin peripheral rim enhancement (arrows). The differential diagnosis includes abscess or biloma. **(c)** Axial Gd-EOB-DTPA–enhanced T1-weighted 3D GRE image obtained 15 hours after injection shows delayed contrast material filling in the multiple cystic lesions (arrow), a finding indicative of an intrahepatic biloma related to a bile duct stricture. **(d)** Image from follow-up cholangiography, performed 1 day after percutaneous transhepatic and endoscopic nasobiliary drainage, shows multifocal accumulation of contrast material (arrows), a finding indicative of bilomas. There is complete obstruction of the common hepatic duct (arrowhead) around the surgical clips.

a.

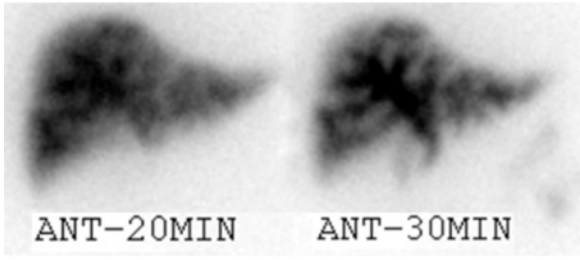

b.

Figure 18. Normal findings in a 45-year-old woman suspected to have sphincter of Oddi dysfunction. **(a)** Coronal multiplanar reformation Gd-EOB-DTPA–enhanced T1-weighted 3D GRE image obtained 30 minutes after injection shows contrast material filling in the bile duct and duodenum (arrow). This finding can help exclude the possibility of sphincter of Oddi dysfunction. **(b)** Images from biliary scintigraphy show a hilum-to-duodenum transit time for the radioactive material of less than 10 minutes, a finding consistent with absence of sphincter of Oddi dysfunction.

Miscellaneous

Differentiation of a Biloma from Other Pathologic Conditions.—A biloma is an encapsulated intrahepatic or extrahepatic bile collection outside the biliary tree that arises due to a bile leak. Differentiation of intrahepatic biloma from other hepatic space-occupying lesions, such as abscess, metastasis, or hematoma, is critical to therapeutic decision making. At Gd-EOB-DTPA–enhanced MR cholangiography, intrahepatic biloma often appears as an intrahepatic fluid collection with delayed contrast agent filling (Fig 17).

Mn-DPDP–enhanced MR cholangiography allows differentiation of extrahepatic biloma from a perihepatic fluid collection of nonbiliary origin by demonstrating contrast material leakage into the extrahepatic biloma (9). As with the use of Mn-DPDP–enhanced MR cholangiography, Gd-EOB-DTPA–enhanced MR cholangiography can also be helpful in the diagnosis of extrahepatic biloma (Fig 13) (9).

Sphincter of Oddi Dysfunction.—Sphincter of Oddi dysfunction is a clinical syndrome of biliary or pancreatic obstructions associated with structural or functional abnormalities of either the biliary or pancreatic sphincter of Oddi, although both types have been associated with biliary pain and pancreatitis. Although sphincter of Oddi manometry is considered the standard of reference for diagnosis, the associated substantial morbidity of the technique makes it an inappropriate screening test. Therefore, less invasive methods of detecting a delay in bile or pancreatic fluid drainage, such as ERCP or biliary scintigraphy, are preferred for screening (Fig 18) (46).

At conventional T2-weighted MR cholangiography, mild dilatation of the bile duct, pancreatic duct, or both down to the level of the ampulla of Vater and no definite neoplastic or inflammatory conditions in the pancreaticobiliary tracts might be suggestive of sphincter of Oddi dysfunction. However, assessment of delayed drainage is difficult with conventional MR cholangiography.

Therefore, Gd-EOB-DTPA–enhanced MR cholangiography can be used as an alternative imaging tool for establishing the possibility of sphincter of Oddi dysfunction by providing functional information on bile flow dynamics. Delayed passage of bile through the ampulla of Vater might be determined by observing delayed passage or no passage of contrast material in the ampulla of Vater on images usually obtained more than 0.5–1 hour after intravenous injection of Gd-EOB-DTPA. In addition, Gd-EOB-DTPA–enhanced MR cholangiography can be helpful in excluding the possibility of sphincter of Oddi dysfunction by demonstrating normal passage of contrast material in the bile ducts on images obtained after a 20–30-minute delay in patients clinically suspected to have sphincter of Oddi dysfunction (Fig 18) (5,6,16).

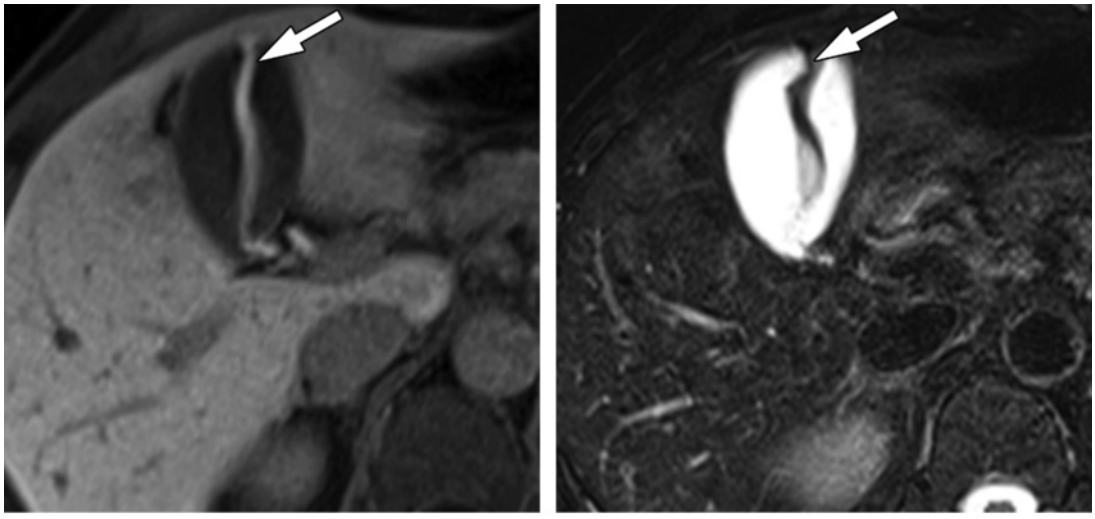

a. b.

Figure 19. T2-shortening effect of concentrated contrast material. **(a)** Axial Gd-EOB-DTPA–enhanced T1-weighted 3D GRE image obtained 10 minutes after injection shows a jet of contrast material in the gallbladder lumen (arrow). **(b)** Axial T2-weighted turbo spin-echo image obtained after Gd-EOB-DTPA administration shows an artifact (arrow) in the gallbladder. The artifact is due to the T2-shortening effect of the concentrated contrast material.

Pitfalls

The excretion of Gd-EOB-DTPA into the biliary tree interferes with successful visualization of biliary fluid at conventional T2-weighted MR cholangiography. At a higher concentration of the contrast material, the signal intensity of bile appears darker on T2-weighted images owing to the T2-shortening effect of concentrated contrast material within the bile ducts. Therefore, conventional MR cholangiography should be performed before excretion of Gd-EOB-DTPA into the biliary tree (Fig 19) (14).

Poor mixing of Gd-EOB-DTPA and preexisting bile can result in pseudo–filling defects. Therefore, the efficacy of Gd-EOB-DTPA–enhanced MR cholangiography in identification of filling defects may be disappointing in comparison with that of thin-section source T2-weighted MR cholangiography (5). At Gd-EOB-DTPA–enhanced MR cholangiography, filling defects might be masked if contrast material completely fills the bile duct, a pitfall similar to the one that occurs during ERCP due to overfilling or superimposition of contrast medium. Moreover, adequate contrast material filling in the bile duct requires liver function that is normal or at least not substantially reduced and a sufficient delay time (5).

Conclusions

The drawbacks of Gd-EOB-DTPA–enhanced MR cholangiography include its high cost and limitations in depicting the biliary system in patients with hepatobiliary dysfunction. Nevertheless, Gd-EOB-DTPA–enhanced MR imaging combined with T2-weighted MR cholangiography has the potential to provide comprehensive information about the biliary system. This approach can be effective in detection of biliary injury, including leakage and stricture, assessment of bile duct obstruction, diagnosis of cholecystitis, and differentiation of biliary from extrabiliary lesions. Moreover, Gd-EOB-DTPA–enhanced MR cholangiography is noninvasive and does not use ionizing radiation. However, its clinical applications have not yet been completely explored, and further investigations are required to determine the utility of Gd-EOB-DTPA–enhanced MR cholangiography in a clinical setting.

References

1. Balci NC, Semelka RC. Contrast agents for MR imaging of the liver. Radiol Clin North Am 2005;43:887–898.
2. Reimer P, Schneider G, Schima W. Hepatobiliary contrast agents for contrast-enhanced MRI of the liver: properties, clinical development and applications. Eur Radiol 2004;14:559–578.

3. Fayad LM, Holland GA, Bergin D, et al. Functional magnetic resonance cholangiography (fMRC) of the gallbladder and biliary tree with contrast-enhanced magnetic resonance cholangiography. J Magn Reson Imaging 2003;18:449–460.
4. Fayad LM, Kamel IR, Mitchell DG, Bluemke DA. Functional MR cholangiography: diagnosis of functional abnormalities of the gallbladder and biliary tree. AJR Am J Roentgenol 2005;184:1563–1571.
5. Sheppard D, Allan L, Martin P, McLeay T, Milne W, Houston JG. Contrast-enhanced magnetic resonance cholangiography using mangafodipir compared with standard T2W MRC sequences: a pictorial essay. J Magn Reson Imaging 2004;20:256–263.
6. Papanikolaou N, Prassopoulos P, Eracleous E, Maris T, Gogas C, Gourtsoyiannis N. Contrast-enhanced magnetic resonance cholangiography versus heavily T2-weighted magnetic resonance cholangiography. Invest Radiol 2001;36:682–686.
7. Lee VS, Krinsky GA, Nazzaro CA, et al. Defining intrahepatic biliary anatomy in living liver transplant donor candidates at mangafodipir trisodium–enhanced MR cholangiography versus conventional T2-weighted MR cholangiography. Radiology 2004; 233:659–666.
8. Kim KW, Park MS, Yu JS, et al. Acute cholecystitis at T2-weighted and manganese-enhanced T1-weighted MR cholangiography: preliminary study. Radiology 2003;227:580–584.
9. Park MS, Kim KW, Yu JS, et al. Early biliary complications of laparoscopic cholecystectomy: evaluation on T2-weighted MR cholangiography in conjunction with mangafodipir trisodium-enhanced 3D T1-weighted MR cholangiography. AJR Am J Roentgenol 2004;183:1559–1566.
10. Hottat N, Winant C, Metens T, Bourgeois N, Deviere J, Matos C. MR cholangiography with manganese dipyridoxyl diphosphate in the evaluation of biliary-enteric anastomoses: preliminary experience. AJR Am J Roentgenol 2005;184:1556–1562.
11. Hamm B, Staks T, Muhler A, et al. Phase I clinical evaluation of Gd-EOB-DTPA as a hepatobiliary MR contrast agent: safety, pharmacokinetics, and MR imaging. Radiology 1995;195:785–792.
12. Reimer P, Rummeny EJ, Shamsi K, et al. Phase II clinical evaluation of Gd-EOB-DTPA: dose, safety aspects, and pulse sequence. Radiology 1996;199: 177–183.
13. Hammerstingl R, Huppertz A, Breuer J, et al. Diagnostic efficacy of gadoxetic acid (Primovist)-enhanced MRI and spiral CT for a therapeutic strategy: comparison with intraoperative and histopathologic findings in focal liver lesions. Eur Radiol 2008;18:457–467.
14. Bollow M, Taupitz M, Hamm B, Staks T, Wolf KJ, Weinmann HJ. Gadolinium-ethoxybenzyl-DTPA as a hepatobiliary contrast agent for use in MR cholangiography: results of an in vivo phase-I clinical evaluation. Eur Radiol 1997;7:126–132.
15. Carlos RC, Hussain HK, Song JH, Francis IR. Gadolinium-ethoxybenzyl-diethylenetriamine pentaacetic acid as an intrabiliary contrast agent: preliminary assessment. AJR Am J Roentgenol 2002;179: 87–92.
16. Carlos RC, Branam JD, Dong Q, Hussain HK, Francis IR. Biliary imaging with Gd-EOB-DTPA: is a 20-minute delay sufficient? Acad Radiol 2002;9: 1322–1325.
17. Tschirch FT, Struwe A, Petrowsky H, Kakales I, Marincek B, Weishaupt D. Contrast-enhanced MR cholangiography with Gd-EOB-DTPA in patients with liver cirrhosis: visualization of the biliary ducts in comparison with patients with normal liver parenchyma. Eur Radiol 2008;18:1577–1586.
18. Dahlstrom N, Persson A, Albiin N, Smedby O, Brismar TB. Contrast-enhanced magnetic resonance cholangiography with Gd-BOPTA and Gd-EOB-DTPA in healthy subjects. Acta Radiol 2007;48: 362–368.
19. Rohrer M, Bauer H, Mintorovitch J, Requardt M, Weinmann HJ. Comparison of magnetic properties of MRI contrast media solutions at different magnetic field strengths. Invest Radiol 2005;40:715–724.
20. Mortele KJ, Ros PR. Anatomic variants of the biliary tree: MR cholangiographic findings and clinical applications. AJR Am J Roentgenol 2001;177:389–394.
21. McMahon AJ, Fullarton G, Baxter JN, O'Dwyer PJ. Bile duct injury and bile leakage in laparoscopic cholecystectomy. Br J Surg 1995;82:307–313.
22. Aduna M, Larena JA, Martin D, Martinez-Guerenu B, Aguirre I, Astigarraga E. Bile duct leaks after laparoscopic cholecystectomy: value of contrast-enhanced MRCP. Abdom Imaging 2005;30:480–487.
23. Hintze RE, Adler A, Veltzke W, et al. Clinical significance of magnetic resonance cholangiopancreatography (MRCP) compared to endoscopic retrograde cholangiopancreatography (ERCP). Endoscopy 1997;29:182–187.
24. Ergen FB, Akata D, Sarikaya B, et al. Visualization of the biliary tract using gadobenate dimeglumine: preliminary findings. J Comput Assist Tomogr 2008; 32:54–60.
25. An SK, Lee JM, Suh KS, et al. Gadobenate dimeglumine-enhanced liver MRI as the sole preoperative imaging technique: a prospective study of living liver donors. AJR Am J Roentgenol 2006;187: 1223–1233.
26. Levy AD, Rohrmann CA Jr, Murakata LA, Lonergan GJ. Caroli's disease: radiologic spectrum with pathologic correlation. AJR Am J Roentgenol 2002; 179:1053–1057.
27. Park MS, Kim BC, Kim T, Kim MJ, Kim KW. Double common bile duct: curved-planar reformatted computed tomography (CT) and gadobenate dimeglumine-enhanced MR cholangiography. J Magn Reson Imaging 2008;27:209–211.
28. Park MS, Yu JS, Lee JH, Kim KW. Value of manganese-enhanced T1- and T2-weighted MR cholangiography for differentiating cystic parenchymal lesions from cystic abnormalities which communicate with bile ducts. Yonsei Med J 2007;48:1072–1074.
29. Trowbridge RL, Rutkowski NK, Shojania KG. Does this patient have acute cholecystitis? JAMA 2003; 289:80–86.

30. Bortoff GA, Chen MY, Ott DJ, Wolfman NT, Routh WD. Gallbladder stones: imaging and intervention. RadioGraphics 2000;20:751–766.
31. Altun E, Semelka RC, Elias J Jr, et al. Acute cholecystitis: MR findings and differentiation from chronic cholecystitis. Radiology 2007;244:174–183.
32. Ziessman HA. Acute cholecystitis, biliary obstruction, and biliary leakage. Semin Nucl Med 2003;33:279–296.
33. Romagnuolo J, Bardou M, Rahme E, Joseph L, Reinhold C, Barkun AN. Magnetic resonance cholangiopancreatography: a meta-analysis of test performance in suspected biliary disease. Ann Intern Med 2003;139:547–557.
34. Prat F, Pelletier G, Ponchon T, et al. What role can endoscopy play in the management of biliary complications after laparoscopic cholecystectomy? Endoscopy 1997;29:341–348.
35. Freeman ML, Overby C. Selective MRCP and CT-targeted drainage of malignant hilar biliary obstruction with self-expanding metallic stents. Gastrointest Endosc 2003;58:41–49.
36. Tantia O, Jain M, Khanna S, Sen B. Iatrogenic biliary injury: 13,305 cholecystectomies experienced by a single surgical team over more than 13 years. Surg Endosc 2008;22:1077–1086.
37. Strasberg SM, Hertl M, Soper NJ. An analysis of the problem of biliary injury during laparoscopic cholecystectomy. J Am Coll Surg 1995;180:101–125.
38. Lau WY, Lai EC. Classification of iatrogenic bile duct injury. Hepatobiliary Pancreat Dis Int 2007;6:459–463.
39. McQuillan T, Manolas SG, Hayman JA, Kune GA. Surgical significance of the bile duct of Luschka. Br J Surg 1989;76:696–698.
40. Thurley PD, Dhingsa R. Laparoscopic cholecystectomy: postoperative imaging. AJR Am J Roentgenol 2008;191:794–801.
41. Lucas MH, Elgazzar AH, Cummings DD. Positional biliary stasis: scintigraphic findings following biliary-enteric bypass surgery. J Nucl Med 1995;36:104–106.
42. Soto JA, Yucel EK, Barish MA, Chuttani R, Ferrucci JT. MR cholangiopancreatography after unsuccessful or incomplete ERCP. Radiology 1996;199:91–98.
43. Pavone P, Laghi A, Catalano C, et al. MR cholangiography in the examination of patients with biliary-enteric anastomoses. AJR Am J Roentgenol 1997;169:807–811.
44. Merkle EM, Boll DT, Weidenbach H, Brambs HJ, Gabelmann A. Ability of MR cholangiography to reveal stent position and luminal diameter in patients with biliary endoprostheses: in vitro measurements and in vivo results in 30 patients. AJR Am J Roentgenol 2001;176:913–918.
45. Nitatori T, Hanaoka H, Hachiya J, Yokoyama K. MRI artifacts of metallic stents derived from imaging sequencing and the ferromagnetic nature of materials. Radiat Med 1999;17:329–334.
46. Petersen BT. Sphincter of Oddi dysfunction, part 2: Evidence-based review of the presentations, with "objective" pancreatic findings (types I and II) and of presumptive type III. Gastrointest Endosc 2004;59:670–687.

Biliary MR Imaging with Gd-EOB-DTPA and Its Clinical Applications

Nam Kyung Lee, MD, et al

RadioGraphics 2009; 29:1707–1724 • **Published online** 10.1148/rg.296095501 • **Content Codes:** GI MR

Page1708
Gd-EOB-DTPA is a highly water-soluble contrast agent in which an ethobenzyl group is attached to gadolinium diethylenetriamine pentaacetic acid. The resulting compound has the properties of a conventional nonspecific extracellular contrast agent but with the additional properties of a hepatocyte-specific agent, thereby allowing improved examination of the hepatobiliary system (1,2,11–18).

Page 1712
MR imaging findings of Caroli disease include multiple intrahepatic cysts in close relation to the biliary system and the presence of the central dot sign (26). However, MR imaging fails to demonstrate communication between cystic lesions and draining bile ducts. This problem could be resolved with Gd-EOB-DTPA–enhanced MR cholangiography, which can demonstrate communications between cystic lesions and draining bile ducts and allows differentiation of Caroli disease from autosomal-dominant polycystic liver disease or peribiliary cysts in a cirrhotic liver (Figs 6, 7) (6,27,28).

Page 1715
However, in our experience, Gd-EOB-DTPA–enhanced MR imaging combined with T2-weighted MR cholangiography could also improve the ability to diagnose acute cholecystitis by providing not only anatomic information such as impacted cystic duct or gallbladder stones, but also functional information on cystic duct obstruction as evidenced by lack of visualization of contrast material filling in the gallbladder, similar to the information provided by Mn-DPDP–enhanced MR imaging (Fig 8) (3,8).

Page 1715
Although the biliary excretion of Gd-EOB-DTPA may be affected by various factors as well as the degree of bile duct obstruction, the degree of bile duct obstruction might be simply classified with delayed Gd-EOB-DTPA–enhanced bile flow dynamics (usually evaluated >30 minutes after intravenous injection of Gd-EOB-DTPA): complete obstruction (absence of contrast agent filling in the distal and even proximal parts of the stricture or obstructive lesion), near-complete obstruction (significantly delayed contrast agent filling only in the proximal part of the stricture or obstructive lesion), and partial obstruction (passage of contrast agent beyond the apparent stricture or obstructive lesion) (Figs 9, 10) (4–6,16).

Page 1717
Gd-EOB-DTPA–enhanced MR cholangiography allows detection of active bile leakage by direct visualization of contrast material extravasating into fluid collections, as well as demonstrating the anatomic site of the leakage and the type of bile duct injury (Figs 3, 12–14) (22,40). Gd-EOB-DTPA–enhanced MR cholangiography is also useful in assessing the degree of any obstruction according to the presence or absence of contrast material downstream in the bile duct (Fig 14).